ACS Sustainable Chemistry & Engineering

pubs.acs.org/journal/ascecg

Research Article

Ionic Liquids–Cobalt(II) Thermochromic Complexes: How the Structure Tunability Affects "Self-Contained" Systems

Floriana Billeci, H. Q. Nimal Gunaratne, Peter Licence, Kenneth R. Seddon, Natalia V. Plechkova, and Francesca D'Anna*

Cite This: *ACS Sustainable Chem. Eng.* 2021, 9, 4064–4075

Read Online

ACCESS | Metrics & More | Article Recommendations | Supporting Information

ABSTRACT: With the aim of obtaining thermochromic systems with potential applications in solar energy storage, we evaluated the behavior of some sugar-based ionic liquids (ILs)–$Co(NTf_2)_2$ complexes, in IL solution, as a function of temperature. Different structural changes on the cation, the nature of the anion, and the nature of the IL used as the solvent were considered. The analysis of the above factors was carried out through a combined approach of different techniques, that is, variable temperature UV–vis and NMR spectroscopies, conductivity, and thermal gravimetric analysis. The thermochromic systems were analyzed both as solutions and as thin films, and the data collected highlight the defining role played by both the cation structure and the solvent nature in determining their performance. Most of the investigated systems show a chromogenic transition from pink to blue, occurring in a temperature range suitable for practical applications (40–60 °C). Interestingly, when embedded in a polymeric matrix, thin films with high recyclability and long life are also described.

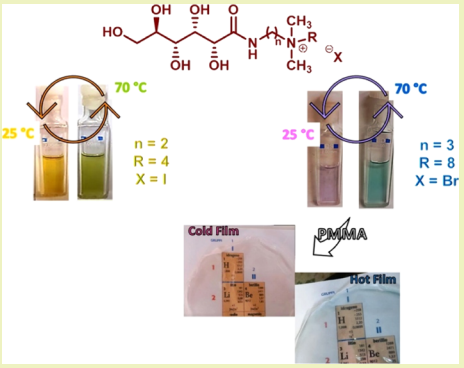

KEYWORDS: *thermochromism, ionic liquids, polymer films, switchable magnetism*

INTRODUCTION

The ever-increasing global energy demands, due to expanding developments and increasing populations, have led to serious scrutiny over the depleting energy resources. Global energy demand has focused attention on sustainable energy generation coupled with optimized use of energy and minimized pollution, limiting fossil fuel-based energy consumption to a bare minimum. These aspects have led to an increasing focus on the short-term stored energy resources, which could be derived from wind power, hydropower, solar power, biomass, and so forth. Solar energy is a viable and inexhaustible source of energy[1] for generating power, with the aid of solar cells, and harnessing its heat *via* efficient storage of sun's heat using compounds/materials with high heat capacities. In relation to this, it is a major challenge to store energy due to daily and seasonal variations in the accessibility of sunlight. The schemes generally known as molecular solar thermal systems, for example, phase-changing materials that store energy in the form of lattice energy, represent a promising avenue for harvesting and storing solar energy.[2−4] In this context, photochromic systems where a molecule is converted by photoisomerization into a higher-energy isomer, which is capable of storing the energy until released by a trigger, converting the metastable isomer to the original light-harvesting isomer,[5−9] have played a significant role.

Thermochromism, defined as reversible change in the color of a compound when it is heated or cooled, has received little attention as an energy harvesting mechanism.[10−12] The thermochromic color change of a compound/material is distinguished often by eye, occurring over a small or sharp temperature interval. For inorganic compounds, this transition is frequently due to a change in the crystalline phase, to a change in ligand geometry, as a result of charge transfer,[13] modifications in the chemical structure,[14] or to a change in the number of molecules of the solvent in the first coordination sphere.[15,16] A fewer known examples are as a result of equilibria between complexes in solution or to equilibria between different molecular structures in the case of organometallic compounds.[17] The thermochromic transition temperature of a pure substance may be greatly changed by dispersing the compound in a solid matrix or by mixing it with other substances. Widely used matrices include waxes and polymers which are compatible with the thermochromic substance. In the solid matrix, a hysteresis effect of color transition may be affected by the nature of the matrix. In this context, thermochromic substances, embedded in coatings, are beginning to surface in the design of new materials for energy

Received: November 24, 2020
Revised: February 10, 2021
Published: March 10, 2021

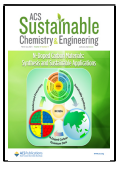

Scheme 1. Structures of the ILs Investigated in This Work

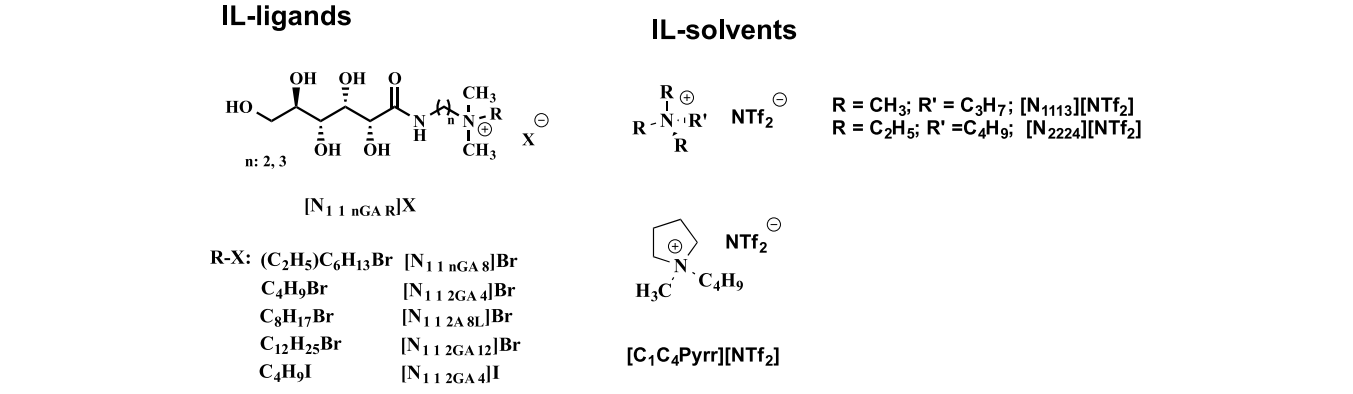

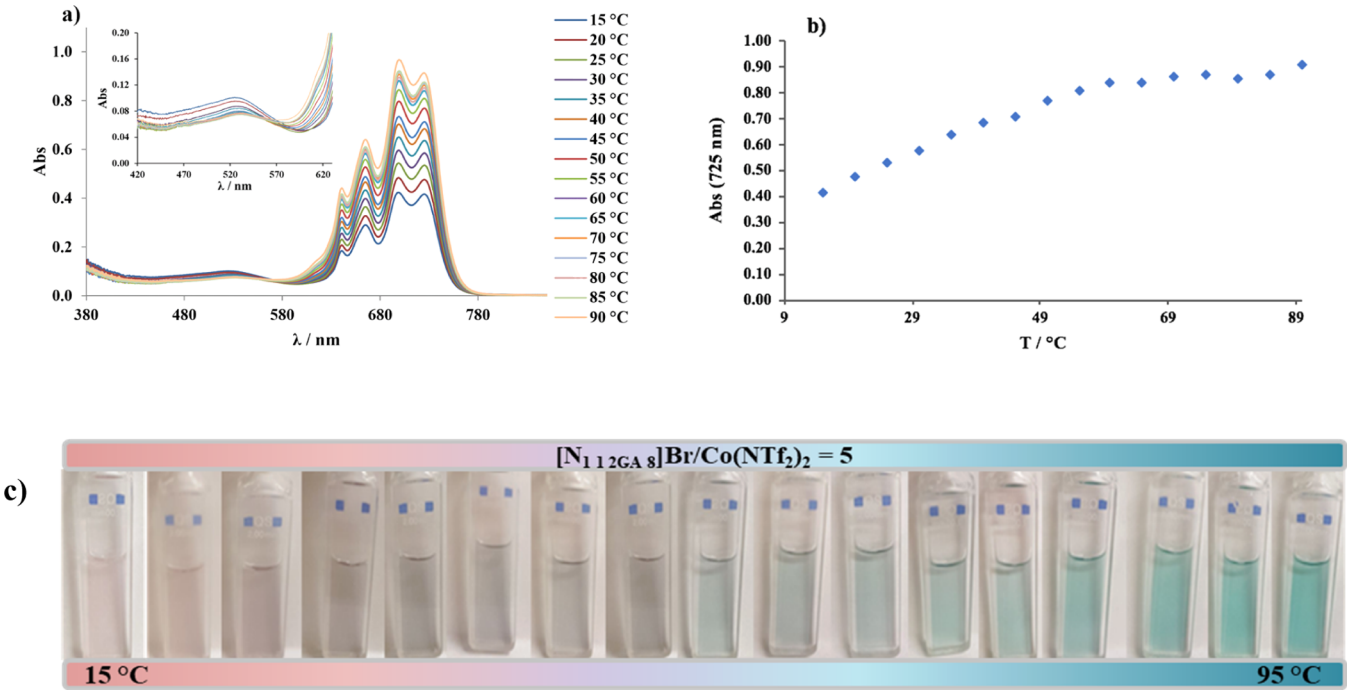

Figure 1. (a) UV−vis spectra of $[N_{1\ 1\ 2\ GA\ 8}]Br/Co(NTf_2)_2/[N_{2224}][NTf_2]$ at a ligand/metal molar ratio equal to 5 (inset: high energy band); (b) trend of absorbance at 725 nm as a function of temperature; (c) color shades.

saving.[18−20] In some cases, the percentage of energy savings reached to more than 16%.[21] Looking specifically at thermochromic transition-metal complexes, the states with different coordination numbers are shown to be in equilibrium with the ligand or solvent molecules where the increase in temperature generally favors the lower-coordinated complex.[22]

Among transition-metal complexes, thermochromism of cobalt is the most widely known and has been studied in different solvent systems.[15,23] Gadzuric *et al.*[33] examined the thermochromic phenomena of cobalt(II) chloride complexes in NH_4NO_3·*z*NMF (*N*-methylformamide) (*z* = 3, 4, 5, 6, and 20) solution, in the temperature range of 33−73 °C, who showed the insertion of chloride ion in the metal coordination sphere, favors the transition from an octahedral to a tetrahedral geometry inducing a color change.[24] However, these kind of systems, involving a ligating volatile solvent, are often not self-contained as the phenomenon depends on the addition or removal of (solvent) ligands, where water is a commonly used solvent.[25] The key challenging issue regarding such thermochromic systems involving metal complexes is the volatility of the solvent used while maintaining a viable temperature range in which the transformation occurs.

In this context, ionic liquids (ILs) present a viable alternative to ligating solvents with their high thermal stability and desirable structure tunability,[24,26] allowing their application in different fields.[27−29] Moreover, the associated anions in ILs can be chosen to adjust coordination capability toward metal ions. In this regard, imidazolium-based ILs have been used in combination with Ni(II) salts, both in solutions and thin films, to obtain systems that show a thermochromic transition from green to blue in the temperature range 35−65 °C or room temperature−120 °C.[30−32] Furthermore, imidazolium ILs have also been used in combination with Co(II) salts, giving systems in which the thermochromic switch occurs under room[33−35] or subzero temperatures or alternatively, at very high temperatures.[35−37] These transition temperatures limit the use such IL−metal complexes within the solar thermal energy range. To overcome such limitations, we have recently introduced a self-contained IL−Co(II) system,[38] where the ILs were synthesized from a sugar-based source (derived from food

https://dx.doi.org/10.1021/acssuschemeng.0c08586
ACS Sustainable Chem. Eng. 2021, 9, 4064−4075

Table 1. Temperature of the Geometry Switch for the System $[N_{1\ 1\ 2GA\ 8}]Br/Co(NTf_2)_2/[N_{2\ 2\ 2\ 4}][NTf_2]$ at Different Ligand/Metal Molar Ratios and Using Different ILs as the Solvent

entry	thermochromic system	ratio [ligand]/[metal]	T_{switch} °C[a]
1	$[N_{1\ 1\ 2GA\ 8}]Br/Co(NTf_2)_2/[N_{2\ 2\ 2\ 4}][NTf_2]$[38]	3:1	59
2	$[N_{1\ 1\ 2GA\ 8}]Br/Co(NTf_2)_2/[N_{2\ 2\ 2\ 4}][NTf_2]$	5:1	56
3	$[N_{1\ 1\ 2GA\ 8}]Br/Co(NTf_2)_2/[N_{2\ 2\ 2\ 4}][NTf_2]$	6:1	82
4	$[N_{1\ 1\ 2GA\ 8}]Br/Co(NTf_2)_2/[N_{2\ 2\ 2\ 4}][NTf_2]$	7:1	55 and 89
5	$[N_{1\ 1\ 2GA\ 8}]Br/Co(NTf_2)_2/[C_1C_{4pyrr}][NTf_2]$	3:1	44
6	$[N_{1\ 1\ 2GA\ 8}]Br/Co(NTf_2)_2/[N_{1\ 1\ 1\ 3}][NTf_2]$	3:1	57

[a] T_{switch} were reproducible within 1 °C.

waste), utilizing a simple reaction scheme. It was found to be compatible with some polymer matrices, allowing the fabrication of composite systems for real-life applications. We hypothesized that solar thermal energy can be absorbed and stored in the high energy state of the thermochromic system, subsequently emitting the stored heat during the return to a low energy state.

Here, we report a detailed investigation of the system examining the thermochromic interactions occurring between sugar-based ILs, acting as ligands, and a cobalt salt, $Co(NTf_2)_2$ (Scheme 1); in particular, IL ligands bear gluconic functionality in the cation structure. The IL ligands, when taken into consideration, differ in the alkyl chain length, varying from butyl to dodecyl chains. In the case of the octyl derivative, the effect of alkyl chain branching was also considered using both linear octyl and a 2-ethylhexyl derivative. Furthermore, cations also differ in the length of the spacer between the amide and ammonium functionalities. As for the anion effect, both bromide and iodide salts were used. The synthesis and toxicological aspects of these IL ligands have been recently investigated, demonstrating that this class of ILs show both low cyto- and ecotoxicities.[39]

IL-based thermochromic systems obtained show transitions in the useful temperature range of 40−60 °C and demonstrate the significant effect that structural changes on the ions exert on their performance. The systems were analyzed both in solution and in polymeric films, opening the way to elucidate the parameters driving the thermochromic systems to suit any prospective applications.

RESULTS AND DISCUSSION

UV−Vis Investigations. As stated above, the system $[N_{1\ 1\ 2GA\ 8}]Br/Co(NTf_2)_2$ (3:1) was previously investigated in $[N_{2\ 2\ \ 2\ 4}][NTf_2]$ solution [from now on, systems will be indicated as IL−ligand/$Co(NTf_2)_2$/IL solvent *n*:1, where *n* indicates the molar ratio ligand/$Co(NTf_2)_2$].[38] The need for using a solvent came from the high viscosity of the IL ligand, which made a direct investigation of the complex more difficult. The solution obtained showed a color transition from pink to blue at 59 °C (T_{switch}), and this change was ascribed to a variation of the complex geometry from octahedral (O_h) to tetrahedral (T_d). The above hypothesis was also confirmed by the determination of the magnetic momentum (μ_{eff}). Furthermore, a previous investigation demonstrated the need to have the presence of the gluconic moiety in the ligand to observe the thermochromic transition.

Bearing in mind the above result, we first investigated the effect of the ligand/metal molar ratio that can potentially affect the establishment of equilibrium. In particular, the above parameter was changed from 1.5 up to 7. Figures 1 and S1−S3 show the UV−vis spectra and the trend of absorbance as a function of the temperature and color shades for the corresponding solutions.

UV−vis measurements were performed in the range 15−90 °C, with the exception of the highest molar ratios (6 and 7), for which a starting temperature of 30 °C was used as a consequence of the opalescence of the solutions observed at low temperature.

It should be noted that at the lowest molar ratio (1.5), a thermoreversible system was not obtained. The suspension, first pink in color, became a clear blue solution after heating, maintaining this color also after cooling. This was confirmed by the absence of variations in the UV−vis spectra with the raise in temperature (Figure S1a).

In all the other cases, spectra show two sets of different bands, the first one located in the range 450−600 nm and the second in the range 600−800 nm. According to previous reports, the band at the lower wavelength is related to the octahedral complex (O_h), whose weak absorption is in line with the Laporte rule.[40] The second high absorption band can be related to the tetrahedral complex (T_d) which, lacking a center of symmetry, featured a strong absorption that can also be related to its concentration. Raising the temperature, a decrease in the intensity of the high-energy band and a corresponding increase in intensity of the low-energy band was observed according to the occurrence of an equilibrium process. The above hypothesis was further supported by the detection of isosbestic points, whose position moved at longer wavelengths as a function of the molar ratio: 550[38]−561−605−633 nm for the molar ratios 3, 5, 6, and 7, respectively. According to a previous report, this hypsochromic shift can be related to the amount of the ligand available in the solution that, in turn, affects the amount of precursor that is converted into the product,[41] inducing a faster and easier formation of the tetrahedral complex.

Analysis of the absorbance values, at 725 nm, as a function of temperature gives the trends reported in Figures 1b and S2. These trends show changes in the slope and the temperatures (T_{switch}, Table 1), obtained by extrapolation, corresponding to the point of intersection of the two straight lines and representing visible changes in the color of the solution due to the O_h−T_d switching.

The increase in the molar ratio affected T_{switch} values. Indeed, the above parameter stayed almost constant, increasing the molar ratio from 3 up to 5 (entries 1−2), but with a further increase in the molar ratio, the above parameter moved T_{switch} to higher values, 82 °C (entry 3) for a ratio of 6 and 55 and 89 °C for the highest ratio (entry 4). Interestingly, in this case, at 55 °C, the solution with the molar ratio (7:1) appeared to be light blue in color, but upon increasing the temperature, it became a deeper blue. Probably, the obtained result can be ascribed to the increase in the viscosity of solution due to the

https://dx.doi.org/10.1021/acssuschemeng.0c08586
ACS Sustainable Chem. Eng. 2021, 9, 4064−4075

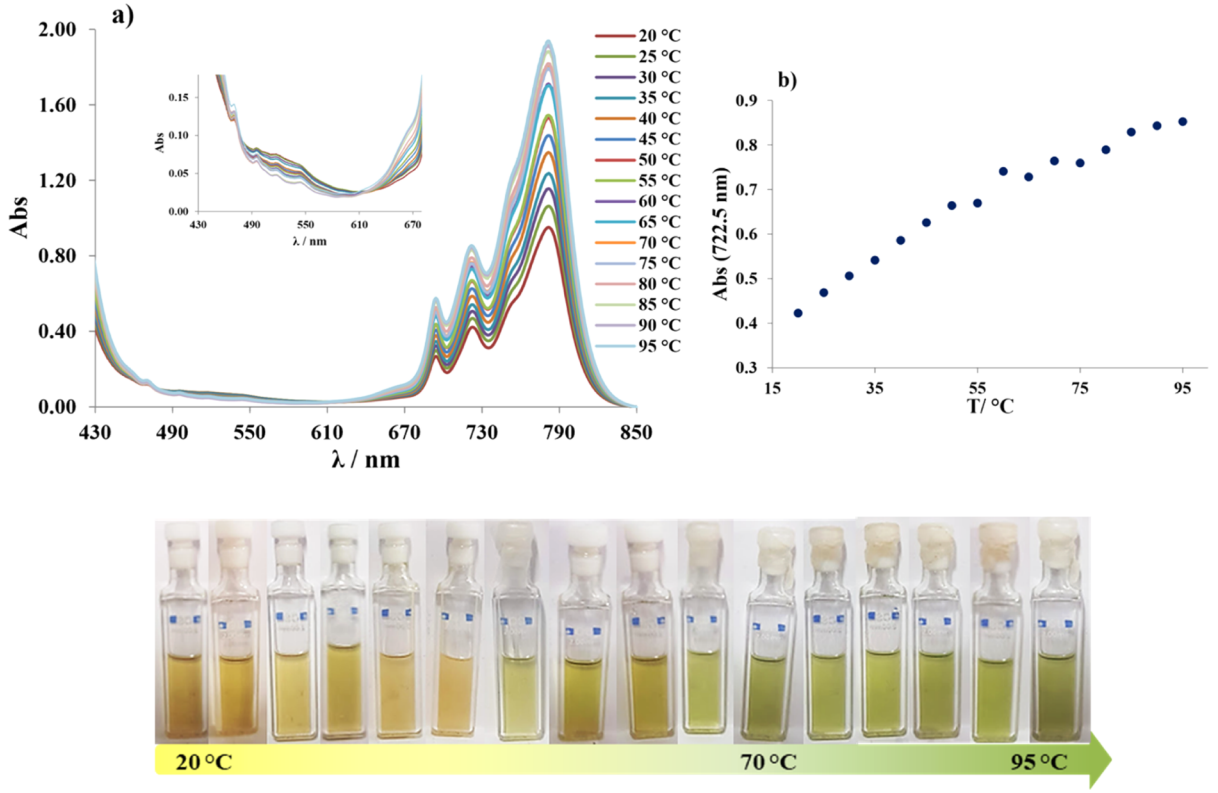

Figure 2. (a) UV−vis spectra (inset: high energy band); (b) trend of absorbance as a function of the temperature; (c) color shades for the system $[N_{1\ 1\ 2GA\ 4}]I/Co(NTf_2)/[N_{2\ 2\ 2\ 4}][NTf_2]$ (3:1).

presence of a larger amount of the ligand, consequently slowing down the establishment of the equilibrium.

Among the analyzed systems, $[N_{1\ 1\ 2GA\ 8}]Br/Co(NTf_2)_2$ with molar ratio (3:1) showed the best performance and it was selected to optimize all the other experimental parameters.

In an attempt to improve system performance, we investigated the effect of solvent nature using $[N_{1\ 1\ 1\ 3}][NTf_2]$ and $[C_1C_4pyrr][NTf_2]$ (Scheme 1). With respect to the previously used IL, $[N_{1\ 1\ 1\ 3}][NTf_2]$ exhibited a lower viscosity (72.0 and 104 cP, at 25 °C, for $[N_{1\ 1\ \ 1\ 3}][NTf_2]$[42] and $[N_{2\ 2\ \ 2\ 4}][NTf_2]$,[43] respectively). On the other hand, $[C_1C_4pyrr][NTf_2]$ had a comparable viscosity to $[N_{1\ 1\ 1\ 3}]$-$[NTf_2]$ (72 cP, at 25 °C)[44] but with a different cation structure. Also, in this case, macroscopic color changes were observed together with significant variations in the UV−vis spectra (Figures S4 and S5). However, in contrast to that which was detected in $[N_{2\ 2\ 2\ 4}][NTf_2]$ solution, in both cases, the band related to the octahedral geometry was less pronounced and the trend of absorbance as a function of temperature showed a more gradual change in the slope.

The analysis of the T_{switch} values (Table 1, entries 4−5) sheds light on the major role played by the IL cation structure, rather than the viscosity. Indeed, the transition temperature stayed unchanged when going from $[N_{2\ 2\ \ 2\ 4}][NTf_2]$ to $[N_{1\ 1\ \ 1\ 3}][NTf_2]$, notwithstanding a decrease in the solvent viscosity. Conversely, it significantly decreased down to 44 °C, changing the solvent from $[N_{1\ 1\ \ 1\ 3}][NTf_2]$ to $[C_1C_4pyrr]$-$[NTf_2]$, despite the lower differences in viscosity. Probably, a cation with a more organized structure and a lower conformational flexibility, such as $[C_1C_4pyrr]^+$, interferes less with the occurrence of changes in the metal coordination sphere that are necessary to favor the transition from the octahedral to the tetrahedral complex. This gives rise to a system more suitable for a practical application, considering that the change in color occurs at a temperature that can be reached during hotter days in the summer.

The last factor we considered was the effect deriving from structural changes on the ligand (cation). On this subject, it is noteworthy that the structural variation may pertain to the length of the spacer between the ammonium and the amide functionalities or the nature (length and branching) of the alkyl chain on the ammonium cation and the anion.

First, we analyzed the effect due to the spacer using the $[N_{1\ 1\ 3GA\ 8}]Br$ (Figure S6a,b). Also in this case, a reversible color change was observed with an isosbestic point at 576 nm that was bathochromically shifted by 30 nm with respect to the one detected in the presence of $[N_{1\ 1\ 2GA\ 8}]Br$.[38]

Interestingly, the change in slope occurred at 45 °C, reflecting a color switch from pink to light blue, but a net gap in the absorbance value was also detected at 79 °C, corresponding to the complete transition to tetrahedral geometry and a blue coloration of the solution. The observed transition accounts for the positive role played by the elongation of the spacer, leading to the increased conformational flexibility, which allows an easier rearrangement of the ligand in the metal coordination sphere.

Further investigation aimed at assessing the effect exerted by the nature of the alkyl chain on the ammonium head, using ligands such as $[N_{1\ 1\ 2\ GA\ 8L}]Br$, $[N_{1\ 1\ 2GA\ 4}]Br$, and $[N_{1\ 1\ 2GA\ 12}]$ Br, gave no pronounced thermochromic effects (Figure S6c−f). Indeed, in all cases, the above structural changes suppressed the thermochromic behavior; a blue solution, representative of the predominance of the tetrahedral complex, was obtained at

https://dx.doi.org/10.1021/acssuschemeng.0c08586
ACS Sustainable Chem. Eng. 2021, 9, 4064−4075

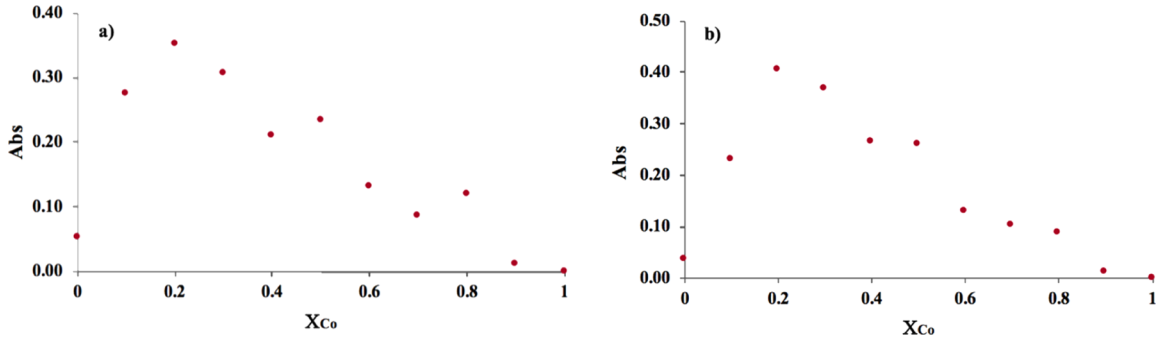

Figure 3. Job plots (ΔA *vs* X_{Co}) for the system $[N_{1\ 1\ 3GA\ 8}]Br/Co(NTf_2)_2/[N_{2\ 2\ 2\ 4}][NTf_2]$ at (a) 25 °C (λ: 712 nm); (b) 70 °C (λ: 713 nm).

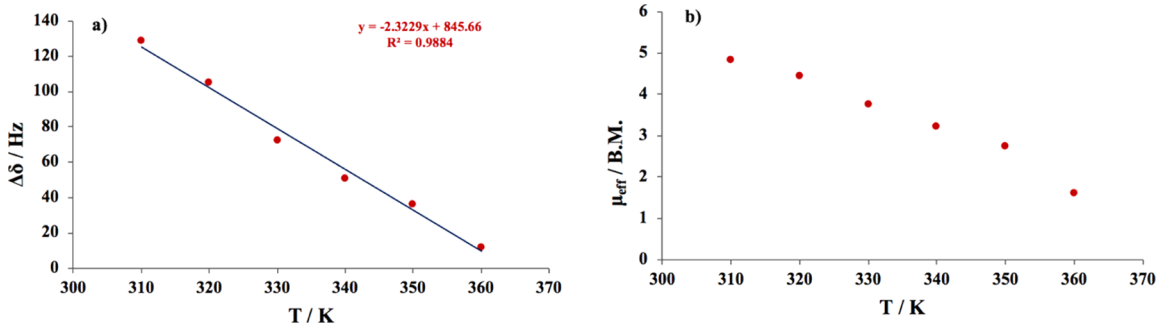

Figure 4. Trends of (a) $\Delta\delta$ as a function of temperature; (b) μ_{eff} as a function of the temperature for the $[N_{1\ 1\ 3GA\ 8}]Br/Co(NTf_2)_2/[N_{2\ 2\ 2\ 4}][NTf_2]$ (3:1)−DMF system.

room temperature and maintained its coloration also after cooling.

Finally, to investigate the role played by the nature of the anionic ligand, we bore in mind results previously collected, demonstrating that changing the bromide ion with a noncoordinating ion, such as $[NTf_2]^-$, suppressed the thermochromic behavior.[38] Consequently, we used an anion having an intermediate coordination ability, such as iodide ion, and using the $[N_{1\ 1\ 2GA\ 4}]^+$ cation, we obtained a yellow solution, which was obtained at room temperature, that gradually turned to green upon increasing the temperature-(Figure 2).

Analysis of the spectra recorded as a function of the temperature shows some interesting features. First, in the region of the tetrahedral complexes, the bands were bathochromically shifted and the one occurring in the range 750−850 nm was quite enlarged. Superimposed spectra allowed the detection of the occurrence of two isosbestic points at 479 and 615 nm. Furthermore, the color change was gradual (Figure 2c) and in the trend of absorbance as a function of temperature (Figure 2b), a change in slope was detected at 55 °C. The above results seem to be indicative of a different interaction between the metal center and the ligand, with respect to the one indicated in the case of $[N_{1\ 1\ 2GA\ 8}]Br$. Probably, the yellow color indicated the first interaction between the "soft" iodide ion and Co(II), further supported by the cooperation of the amide functionalities present on the cation structure. According to previous reports in the literature,[45,46] the color transition from yellow to green could be ascribed to the reorganization in the cobalt coordination sphere, in which the cation participation becomes predominant through a more significant involvement of amide groups. In order to verify that change in color was not due to the formation of I_3^-, a sample of the thermochromic system was added with an equimolar amount of NaSCN. After heating and cooling, the resulting sample retained its thermochromic behavior, effectively eliminating the suggested presence of an iodide complex.

UV−vis investigation was also used to obtain insights on the complex stoichiometry. To this aim, Job's plots were obtained for $[N_{1\ 1\ 2GA\ 8}]Br/Co(NTf_2)_2/[N_{2\ 2\ 2\ 4}][NTf_2]$ and $[N_{1\ 1\ 3GA\ 8}]Br/Co(NTf_2)_2/[N_{2\ 2\ \ 2\ 4}][NTf_2]$ on the grounds of their relatively low transition temperatures.

Measurements were performed both at 25 and 70 °C and the trend of absorbance as a function of the Co(II) mole fraction (X_{Co}) are reported in Figures 3 and S7.

Analysis of the above plot reveals some interesting features. First, the two ligands exhibit different binding abilities, as accounted for by the different shape of the obtained plots. In particular, according to previous reports,[47] in the case of $[N_{1\ 1\ 3GA\ 8}]Br$, a sharp plot was obtained (Figure 3), while for $[N_{1\ 1\ 2GA\ 8}]Br$ a bell-shaped curve was recorded (Figure S7), accounting for a strong binding ability in the first case, more so than in the second case.

In the case of $[N_{1\ 1\ 3GA\ 8}]Br/Co(NTf_2)_2$, the position of the maximum was at $\sim X_{Co}$ = 0.25, indicating a metal/ligand 1:3 stoichiometric ratio. Contrarily, for $[N_{1\ 1\ 2GA\ 8}]Br/Co(NTf_2)_2$, the maximum of the Job's plot occurred at $\sim X_{Co}$ = 0.3, accounting for a 1:2 stoichiometric ratio.

The maximum position did not change by rising the temperature, indicating that the thermochromic behavior is not related to a change in the number of the ligand molecules involved in the complex but rather to the number and nature of chemical functionalities borne on the ligand participating in the interaction.

Magnetic Susceptibility Investigations. The systems obtained were also characterized from a magnetic point of view, determining the magnetic susceptibility. In the case of transition-metal complexes, this kind of investigation provides

https://dx.doi.org/10.1021/acssuschemeng.0c08586
ACS Sustainable Chem. Eng. 2021, 9, 4064−4075

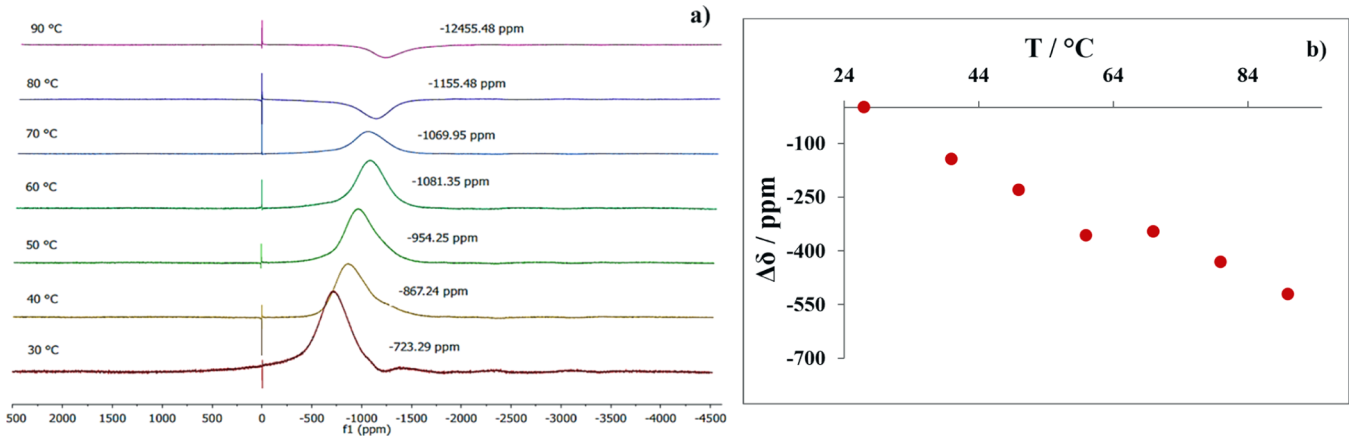

Figure 5. VT ^{59}Co NMR for the system $[N_{1\ 1\ 2GA\ 8}]Br/Co(NTf_2)_2/[N_{2\ 2\ 2\ 4}][NTf_2]$ (7:1) (a) spectra recorded in the range 30−90 °C (^{59}Co signal for $K_3[Co(CN)_6]$ fixed at 0 ppm); (b) trend of $\Delta\delta$ as a function of the temperature in the range 30−90 °C.

information about the complex geometry as the distribution of unpaired electrons in the d-orbitals determines the properties of the complex formed.[48]

To this aim, the Evans method is an indirect method to calculate the magnetic moments (μ_{eff}) through magnetic susceptibility[49] on the grounds of the magnetic response of a probe compound in the presence and absence of the sample (see Supporting Information for details).

This kind of investigation was previously performed on the $[N_{1\ 1\ 2GA\ 8}]Br/Co(NTf_2)_2/[N_{2\ 2\ 2\ 4}][NTf_2]$ (3:1) system and confirmed the interconversion between the octahedral and tetrahedral complexes induced by the increase in temperature.[38]

With the above information in mind, we first investigated the $[N_{1\ 1\ 3GA\ 8}]Br/Co(NTf_2)_2/[N_{2\ 2\ 2\ 4}][NTf_2]$ (3:1) system, using *t*-butanol as the probe, as reported earlier.[38] Unfortunately, after the *t*-butanol addition, the solution became immediately blue and the calculated μ_{eff} values at different temperatures (Table S1) stayed almost constant (Figure S8a,b).

Different results were collected using DMF as the probe compound. Indeed, in this case, the raise in temperature produced a significant difference in the chemical shift ($\Delta\delta$) and produced a variation in the μ_{eff} values (Figure 4).

The magnetic moment gradually decreased, raising the temperature and affecting the values collected up to 40 °C, perfectly accounting for an octahedral geometry (Table S1). However, further increases in temperature induced a significant decrease in μ_{eff}, becoming similar to those obtained using *t*-butanol as a probe compound; this, according to previous reports,[50,51] is indicative of a tetragonal distortion of the original geometry.

The investigation was also performed in the presence of $[N_{1\ 1\ 3GA\ 4}]I$ and the data collected confirmed that the yellow to green color transition corresponded to an octahedral−tetrahedral geometry interconversion (Figure S8c,d). The values obtained (Table S2) match with the high-spin complexes with an electronic distribution for the octahedral geometry $t_{2g}^5e_g^2$ that corresponds to the ground term ^4T. Increasing the temperature, the tetrahedral geometry reorganization determines the electronic configuration $e^4t_2^3$, for a ground term ^4A.[52] Interestingly, the μ_{eff} corresponding to a tetrahedral geometry was obtained at 70 °C, in perfect agreement with the macroscopic color change and UV−vis investigation.

NMR Investigations. The thermochromic systems were further analyzed taking advantage of the magnetic active nature of cobalt. Indeed, ^{59}Co NMR has been widely used to investigate a wide range of different complexes, irrespective of the quadrupolar spin number of cobalt (S = 7/2) that frequently gives a broad peak, which is difficult to observe.[53,54]

In general, changes in the structure of cobalt complexes due to internal or external factors, above all if induced by the temperature, affect the chemical shift values. On this subject, Ozvat *et al.* took advantage of the correlation between the ^{59}Co chemical shift and temperature to perform thermometry *via* magnetic resonance imaging.[55] They investigated $\Delta\delta/\Delta T$ for nuclei of low-spin Co(III) complexes, correlating the degree of ligand encapsulation within the first coordination sphere with the amplification of temperature sensitivity.

The variable temperature (VT) ^{59}Co NMR investigation was performed in the temperature range 30−90 °C, in line with the VT UV−vis measurements. Chemical shift values (δ) were collected using the diamagnetic external standard $K_3[Co(CN)_6]$ having a formal charge on cobalt equal to +3. The external standard exhibits changes in chemical shift as a function of the temperature with a coefficient of 6.2 Hz °C^{-1}.[56] However, changes in chemical shift for the systems investigated were 3 orders of magnitude larger than the ones for the reference signal, avoiding the need to consider corrections to the chemical shift values for the samples.

Data previously collected for $[N_{1\ 1\ 2GA\ 8}]Br/Co(NTf_2)_2/[N_{2\ 2\ 2\ 4}][NTf_2]$ (3:1) shed light on the perfect correspondence between T_{switch} detected by UV−vis investigation and the change in slope occurring in the trend of $\Delta\delta$ as a function of the temperature, supporting the hypothesis that macroscopic color changes can be ascribed to change in the structure of the complex.[38] Now, the effect of the amount of the ligand was taken in consideration, using a ligand/metal molar ratio equal to 7 (Figure 5).

Analysis of NMR spectra accounts for the significant change in chemical shift with the temperature increase. Interestingly, upon raising the temperature, an upfield shift was detected with an inversion of the phase of the signal in the range 70−80 °C. On the other hand, the trend of $\Delta\delta$ as a function of temperature exhibited a plateau region in the range 60−70 °C, in perfect agreement with data collected by UV−vis investigation.

https://dx.doi.org/10.1021/acssuschemeng.0c08586
ACS Sustainable Chem. Eng. 2021, 9, 4064−4075

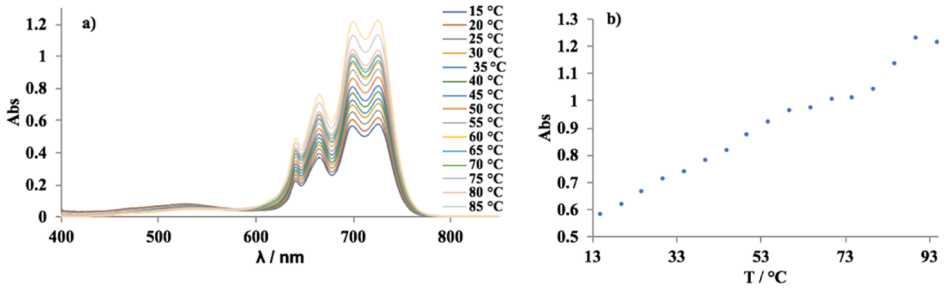

Figure 6. VT UV−vis measurement for the polymeric film $[N_{1\ 1\ 3GA\ 8}]Br/Co(NTf_2)_2$/PMMA (3:1) (390 mg; 84% of PMMA): (a) spectra in the range of temperature 20−90 °C; (b) trend of the absorbance increasing the temperature.

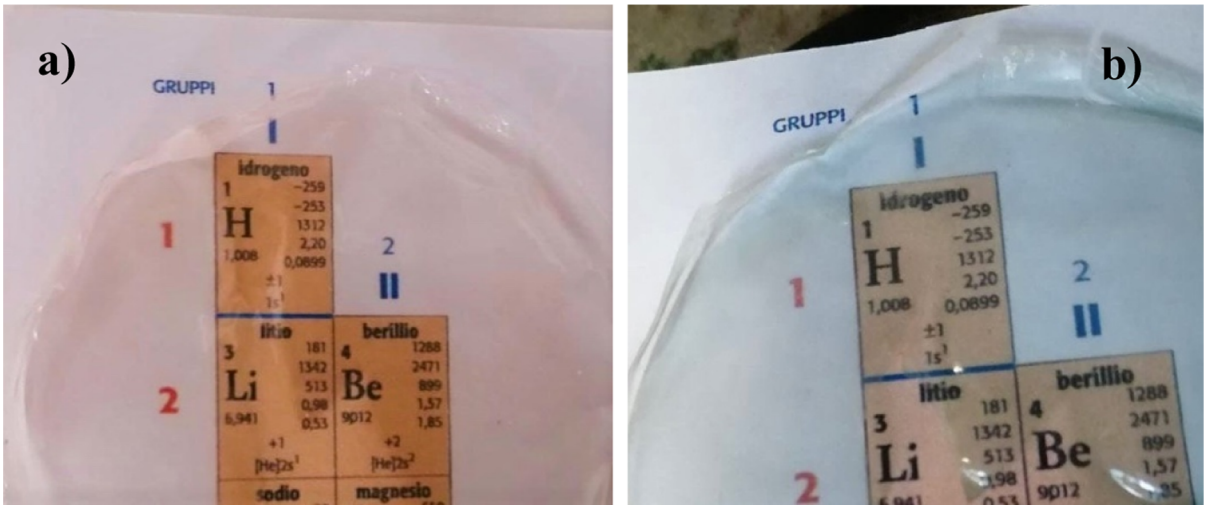

Figure 7. Thermochromic polymeric film $[N_{1\ 1\ 3GA\ 8}]Br/Co(NTf_2)_2$/PMMA (3:1) (390 mg): (a) 25; (b) 80 °C.

To have insights on the effect exerted by the different structural features, the investigation was carried out on $[N_{1\ 1\ 3GA\ 8}]Br/Co(NTf_2)_2$ and $[N_{1\ 1\ 2GA\ 4}]I/Co(NTf_2)_2$ (3:1) (Figure S9). In all cases, an upfield shift of the ^{59}Co signal with the temperature increase was detected. $\Delta\delta$ values show changes in the slope in temperature ranges perfectly matching the ones detected in the UV−vis investigation, confirming that the occurrence of the color change was due to variations in the metal coordination sphere.

Thermochromic Films. The main aim of this work was to verify if the systems obtained could be deployed as components for energy-storage devices. This goal can be achieved by using thin films, and currently, this aim is an open research topic. On this regard, Xu *et al.*[57] developed a nanocomposite hydrogel thermochromic film using pyridinium-modified polyacrylamide networks integrating with EGP5 (ethylene glycol-modified pillar[5]arene) and ATO nanoparticles (antimony−tin oxide). The system was featured by a transition temperature of 32.1 °C and the presence of a polymeric component to avoid the collapse of the hydrogel structure, conferring to the system repeatability and durability.[57] In the same way, Salamati *et al.* used a sol−gel method to dope with W^{6+} ions and TiO_2 a PVP−VO_2 film, which was both thermochromic and photochromic.[58]

Among the factors affecting the performance of thin films, the concentration of the components plays a pivotal role. In this regard, Liu *et al.* incorporate carbon nanotubes (CNTs) in polyethylene terephthalate (PET), obtaining a film whose response time to thermal solicitation was dependent on the quantities of CNT and PET.[59]

With the above information in mind, we considered the system $[N_{1\ 1\ 2GA\ 8}]Br/Co(NTf_2)_2$ (3:1) and prepared thin films, gradually decreasing the amount of PMMA (from 340 down to 290 mg; the mass fraction of polymer in the thin film ranged from 85 down to 81%). In all cases, we obtained homogeneous films showing different thermochromic performance. Indeed, registration of the UV−vis spectra, as a function of temperature, evidences a gradual increase in the spectra baseline at lower wavelengths. However, the bands corresponding to the tetrahedral complex (600−800 nm) were well defined (Figures S10 and S11) and the trends of absorbance as a function of temperature showed a change in slope at around 40 and 55 °C for films prepared in the presence of 83 and 81% of PMMA. In contrast to data previously reported,[38] where the PMMA had a negligible effect on the thermochromic transition, here, the polymer significantly influenced features, as the films became less transparent (Figures S10 and S11).

The same investigation was also performed on the system $[N_{1\ 1\ \ 3GA\ 8}]Br/Co(NTf_2)_2$ (3:1), with the polymer mass fraction ranging from 84 down to 81%. UV−vis spectra and the trend of absorbance as a function of the temperature are reported in Figure 6.

The absorbance of the polymeric film was much lower than the one detected in solution (Figure 6). However, the trend of absorbance as a function of the temperature perfectly agrees with the ones obtained in solution, showing a change in the slope occurring at around 50 °C (Figure 6b) and confirming that also in this case, thermochromic performance was retained in the polymer film. Furthermore, the film was transparent both at 25 and 80 °C but different in color (Figure 7).

https://dx.doi.org/10.1021/acssuschemeng.0c08586
ACS Sustainable Chem. Eng. 2021, 9, 4064−4075

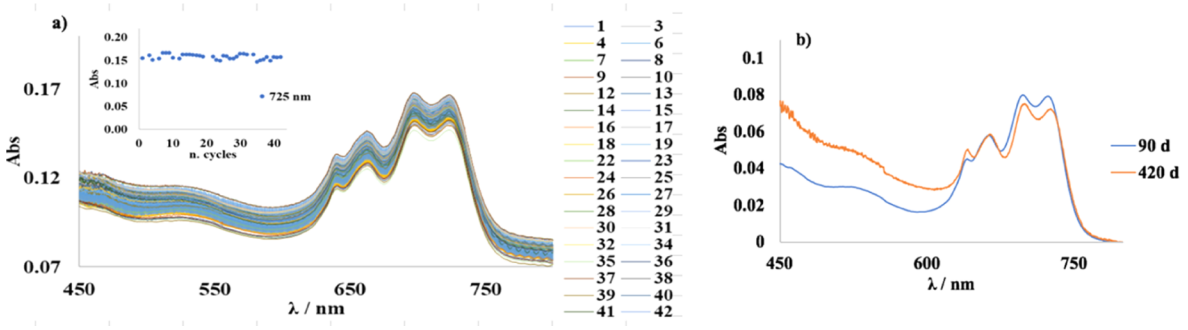

Figure 8. (a)UV−vis spectra recorded for $[N_{1\ 1\ 3GA\ 8}]Br/Co(NTf_2)_2$ (3:1)/PMMA film at 60 °C (inset: absorbance at 725 nm as a function of the number of cycles); (b) UV−vis spectra after 90 and 420 days.

The amount of PMMA was changed using both 83 and 81% of polymers (Figures S12 and S13). The decrease in the polymer amount led to nonhomogeneous and less transparent films, without affecting the thermochromic transition that always occurred in the 55−60 °C range. However, as transparency is a qualification for this kind of systems, the better-performing systems were clearly the ones containing the highest amount of polymer (85 and 84% of PMMA for $[N_{1\ 1\ \ 2\ GA8}]Br/Co(NTf_2)_2$ and $[N_{1\ 1\ \ 3\ GA8}]Br/Co(NTf_2)_2$, respectively).

Bearing in mind this information, we assessed the reusability of the film obtained using the thermochromic complex $[N_{1\ 1\ \ 3\ GA8}]Br/Co(NTf_2)_2$ (3:1). Indeed, possible recycling and long-term life are essential features for such kind of thermochromic coatings. The thin film was heated to 60 °C, and UV−vis spectra were recorded. Interestingly, we were able to reuse the film for 42 cycles over 3 months, without any loss in performance (Figure 8).

To our surprise, after storage in air for 420 days after the last cycle, the UV−vis spectrum did not show significant variations, further supporting the suitability of such a system in a real application.

The above films were consequently investigated for their thermal stability as thermal degradation can occur as a consequence of the stress of the material due to the consecutive heating−cooling cycles. Thermograms for neat polymer and thin polymeric films are displayed in Figure S14, while temperatures corresponding to a 5% of weight loss (T_d) are reported in Table 2.

Table 2. Temperature of Degradation (T_d) Corresponding to the 5% of Weight Loss for the PMMA and the Films Casted

film	T_d (°C)
PMMA	290
$[N_{1\ 1\ 2GA\ 8}]Br/Co(NTf_2)_2$/PMMA	238
$[N_{1\ 1\ 3GA\ 8}]Br/Co(NTf_2)_2$/PMMA	276

In general, the incorporation of the thermochromic systems in the polymeric matrix induces a decrease in the thermal stability with respect to PMMA. Our thermochromic films were stable at temperatures higher than 200 °C, warranting their practical applications, also considering that their color transition occurs at much lower temperatures. Interestingly, the data collected indicate that the thermal stability is affected by the nature of the thermochromic system, with the ones incorporating $[N_{1\ 1\ \ 3GA\ 8}]Br/Co(NTf_2)_2$ (3:1) in PMMA exhibiting the highest thermal stability.

Conductivity Measurements. To have insights on the effect of the ligand structure on the conductivity of the systems, an investigation was performed on both the thermochromic solutions and the films. In particular, the two ligands showing the most interesting behavior were considered, namely, $[N_{1\ 1\ 2GA\ 8}]Br$ and $[N_{1\ 1\ 3GA\ 8}]Br$. The conductivity (σ) was determined through potentiostatic measurements, and these were carried out as a function of the temperature, covering the range 25−70 °C, to obtain information about the contribution deriving from the presence of the octahedral or tetrahedral complex. In all cases, besides the thermochromic system, contributions derived from using IL as a solvent and ligand in IL solution were considered and, in the case of the complex system, a (3:1) ligand/metal stoichiometric ratio was used. Data collected as a function of temperature are shown in Figure 9.

Interestingly, thermochromic systems retain conductive behavior typical of an IL solvent, and both at 25 and 40 °C, σ values for thermochromic solutions were comparable to that of an IL solvent. At 70 °C, a different situation was recorded as the system showed σ values significantly higher than the ones detected for the IL solvent or ligand solution.

However, in the presence of $[N_{1\ 1\ \ 2GA\ 8}]Br$, the above increase seems to be due to an increase in σ value corresponding to the ligand. Conversely, for $[N_{1\ 1\ 3GA\ 8}]Br$, it can be reasonably argued that this is a peculiar feature of the thermochromic system.

Data relevant to the thermochromic films prepared with 85 and 84% of PMMA are reported in Figure 10, together with σ values corresponding to PMMA.

In general, contrary to what was detected in the solution, the increase in temperature does not affect the conductivity values. Obviously, thermochromic systems exhibit higher conductivity values than the PMMA polymer, but in this case, a significant contribution derived from the ligand nature was detected, as accounted for by the higher values measured for $[N_{1\ 1\ 2GA\ 8}]Br/Co(NTf_2)_2$/PMMA (3:1) than for $[N_{1\ 1\ \ 3GA\ 8}]Br/Co(NTf_2)_2$/PMMA (3:1).

CONCLUSIONS

The search for new smart materials to be applied in energy saving is a topic of current interest, with the aim to decrease modern societies' dependency on fossil fuels. The efficiency and environmental impact of the components are imperative in designing such kind of materials.

https://dx.doi.org/10.1021/acssuschemeng.0c08586
ACS Sustainable Chem. Eng. 2021, 9, 4064−4075

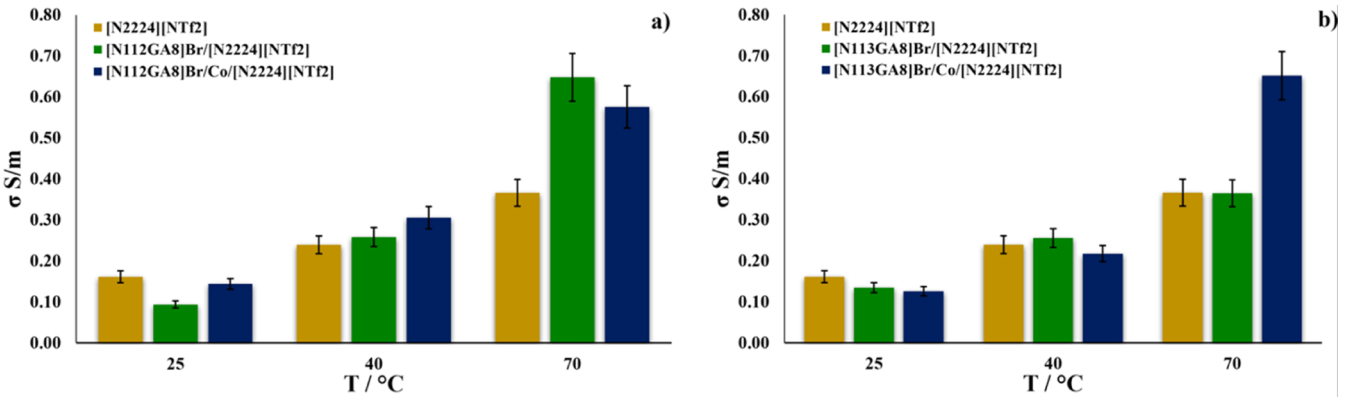

Figure 9. Conductivity (σ) values as a function of the temperature for thermochromic solutions and their components. (a) $[N_{1\ 1\ 2GA\ 8}]Br/Co(NTf_2)_2/[N_{2\ 2\ 2\ 4}][NTf_2]$ (3:1). The film contains 85% of PMMA; (b) $[N_{1\ 1\ 3GA\ 8}]Br/Co(NTf_2)_2/[N_{2\ 2\ 2\ 4}][NTf_2]$ (3:1). The film contains 84% of PMMA.

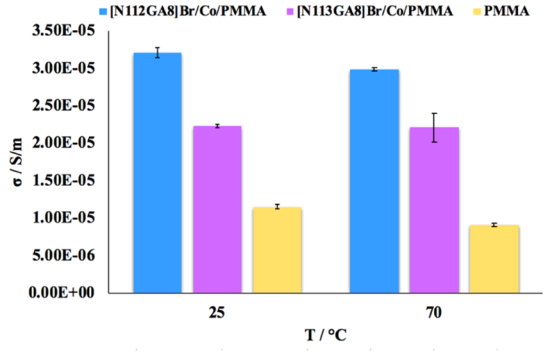

Figure 10. Conductivity (σ) values at variable temperature for PMMA layer and thermochromic films: $[N_{1\ 1\ 2GA\ 8}]Br/Co(NTf_2)_2$/PMMA (3:1) (85% of PMMA) and $[N_{1\ 1\ 3GA\ 8}]Br/Co(NTf_2)_2$/PMMA (3:1) (84% of PMMA).

With the above premises in mind, we analyzed the thermochromic interaction between Co(II) and some sugar-based ILs recently synthesized.[39] Our investigation demonstrated how the right modulation of the IL ligand structure can be the key point to obtain self-containing systems exhibiting thermochromic behavior in a mild range of temperature that goes from 45 up to 59 °C, changing the ligand structure and the solvent nature. These systems exhibit a change in color from pink to light blue, ascribable to a change in the cobalt coordination sphere from octahedral to tetrahedral, as accounted for by the VT NMR and the magnetic susceptibility investigation.

Interestingly, the thermochromic behavior was also retained when the cobalt complex was embedded in a PMMA polymeric matrix, obtaining thin films. The latter retained their conductive properties, which is generally a feature of IL-based systems, but contrary to the corresponding solutions, conductivity values were not affected by temperature. The performance of the films improved in parallel to the increased polymer count. An investigation performed on the recycling of the thin films demonstrated that the $[N_{1\ 1\ 3GA\ 8}]Br/Co(NTf_2)_2$ (3:1)/PMMA film can be reused for 42 cycles over 3 months, without any loss in performance and also after 420 days of storage in air. The performance of these systems has led us to believe that besides the application of the technology in smart windows, they could be also used as coatings in automotive glass or eyeglasses.

The aim of understanding more about the modulation of the thermochromic behavior of cobalt systems with ILs as ligands has been achieved. All of these results could be beneficial to the design of new ligands for smart materials in future applications, opening the possibility of obtaining self-contained thermochromic systems with the aim of reducing the use of carbon sources and environmental preservation. With this in mind and if the IL ligands proved to be eco- and biocompatible,[39] the overall environmental impact of the systems depends also on the nature of the IL used as the solvent, the metal salt used, and the performance as measured in a real apparatus. These are clearly aspects to be investigated and improved in the future to maximize the advantages coming from the systems' resilience.

On this subject, the ligand structure, rich in hydrogen bonds and van der Waals interaction sites, could offer an opportunity to entrap the thermochromic complex in a soft material matrix, such as a gel phase, which could reduce or avoid the leaching issues that sometimes occurs in these types of systems. This could be used as the basis for further study in this area.

EXPERIMENTAL SECTION

Materials. Poly(methyl methachrylate), $[N_{2\ 2\ 2\ 4}][NTf_2]$ (99.0%), $[C_1C_4pyrr][NTf_2]$ (≥98.5%), $[N_{1\ 1\ 1\ 3}][NTf_2]$ (>98.0%), $Co(NTf_2)_2$, and potassium chloride, 0.117 M (conductivity standard) were purchased and used without further purification. $[N_{112GA8}]Br$, $[N_{112GA8L}]Br$, $[N_{113GA8}]Br$, $[N_{112GA12}]Br$, and $[N_{112GA4}]I$ were synthesized according to a previously reported procedure.[39] ILs and ligands were dried under high vacuum at 60 °C before the use. Dichloromethane (DCM, >99.8%) was purchased and used without further purification.

Preparation of the Thermochromic Solution. $Co(NTf_2)_2$ salt (5.75 mg, 9.28×10^{-3} mmol) was dissolved in an IL (600 mg). In order to assist solubilization, the suspension was sonicated with an ultrasound bath (VWR ultrasonic cleaning bath and Decon Ultrasonics Ltd.), working at 45 kHz, for 30 min. A pink homogeneous solution was obtained, to which the proper IL−ligand at the desired molar ratio was added. The mixture was heated at 90 °C for 1.5 h.

Preparation of the Thermochromic Film. The proper ligand (0.11 mmol) and $Co(NTf_2)_2$ (23 mg, 0.037 mmol) were solubilized in DCM (3 mL). The polymer (390/340/290 mg) was solubilized in DCM (8 mL). In order to obtain homogeneous solutions, the mixtures were sonicated for 30 min. After cooling to room temperature, they were mixed, obtaining a pink solution. This solution was placed in a Petri dish (diameter: 10 cm). The solvent slowly evaporated at room temperature. A pink homogeneous film

https://dx.doi.org/10.1021/acssuschemeng.0c08586
ACS Sustainable Chem. Eng. 2021, 9, 4064−4075

was obtained that was subsequently removed from the glass by peeling. The films contained the mass fraction of PMMA ranging from 85 down to 81% for $[N_{112GA8}]Br/Co(NTf_2)_2$ and from 84 down to 81% for $[N_{113GA8}]Br/Co(NTf_2)_2$.

UV−Vis Measurements. UV−vis spectra of the solutions were recorded with a Beckman Coulter DU 800 spectrophotometer, equipped with a Peltier temperature controller. The solution was placed in a quartz cuvette with a light path of 0.2 cm. The spectra were recorded in the wavelength range 250−900 nm. The spectra of the film were recorded using an Agilent Cary 60 UV−Vis spectrophotometer equipped with a temperature control block, where a quartz cuvette, having a light path of 0.2 cm and containing the film, was placed. The spectra were recorded in the wavelength range 300−800 nm.

Preparation of the Sample for the Evans Method.[49] The thermochromic solution was prepared according to the procedure described above. *t*-butanol or DMF (0.2 mL) was added to the solution, and the obtained mixture was transferred into an NMR tube. Additionally, two coaxially capillaries containing the solvent reference (*t*-butanol/DMF and DMSO-d_6) were placed inside the NMR tube. The X_m and the μ_{eff} were calculated using the procedure reported in Supporting Information.

NMR Measurements. The VT ^{59}Co NMR were recorded using the Ascend 600 Bruker with an internal reference solvent ($K_3[Co(CN)_6]$ in D_2O in a sealed silica capillary). Spectra were recorded from 293.15 to 363.15 K, with a temperature gradient of 10 K. Before each measurement, the sample was equilibrated for 20 min.

The VT ^{1}H NMR spectra for the Evans method were recorded using two internal reference solvents (DMSO-d_6 and *t*-butanol/DMF). Also, in this case, before each measurement, the sample was equilibrated for 20 min. A temperature gradient of 10 K was used.

Thermogravimetric Analysis. Thermogravimetric analysis was performed using TA instrument Discovery thermogravimetric analyzer. Samples were placed in a platinum HT pan and heated at a rate of 5 °C min^{-1} under a dinitrogen atmosphere. The onset of weight loss in each thermogram was used as a measure of the decomposition temperature (point at 5 wt % loss of the sample).

Conductivity Measurements. The electrical conductivities σ (S/m) of thermochromic solutions and films were measured with an Autolab potentiostat. The electrochemical impedance spectroscopy measurements were performed applying 0.01 V potential bias to the cell, with frequencies varying from 1×10^5 to 0.1 Hz. The resistance of each sample was determined through the Nyquist plot.[60] The cell constant K for the liquid cell was calculated using a standard solution of KCl. The cell constant for the film cell was calculated experimentally using the cell size and the thickness of the polymer film.

■ ASSOCIATED CONTENT

Supporting Information

The Supporting Information is available free of charge at https://pubs.acs.org/doi/10.1021/acssuschemeng.0c08586.

Magnetic susceptibility calculations, conductivity data, VT UV−vis spectra, and color shades for thermochromic solutions, VT NMR investigations, Job's plots, and VT UV−vis spectra for thermochromic films (PDF)

■ AUTHOR INFORMATION

Corresponding Author

Francesca D'Anna − *Dipartimento STEBICEF, Università degli Studi di Palermo, 90128 Palermo, Italy;* orcid.org/0000-0001-6171-8620; Email: francesca.danna@unipa.it

Authors

Floriana Billeci − *Dipartimento STEBICEF, Università degli Studi di Palermo, 90128 Palermo, Italy; The QUILL Research Centre, School of Chemistry and Chemical Engineering, Queen's University of Belfast, Belfast, Ireland BT9 5AG, U.K.*

H. Q. Nimal Gunaratne − *The QUILL Research Centre, School of Chemistry and Chemical Engineering, Queen's University of Belfast, Belfast, Ireland BT9 5AG, U.K.; School of Chemistry and Chemical Engineering, Queen's University of Belfast, Belfast, Ireland BT9 5AG, U.K.;* orcid.org/0000-0002-4392-8322

Peter Licence − *GSK Carbon Neutral Laboratories, School of Chemistry, The University of Nottingham, Nottingham NG7 2RD, U.K.;* orcid.org/0000-0003-2992-0153

Kenneth R. Seddon − *The QUILL Research Centre, School of Chemistry and Chemical Engineering, Queen's University of Belfast, Belfast, Ireland BT9 5AG, U.K.; Welcome-Wolfson Institute for Experimental Medicine, School of Medicine, Dentistry and Biomedical Sciences, The Queen's University Belfast, BT9 7BL Belfast, U.K..*

Natalia V. Plechkova − *The QUILL Research Centre, School of Chemistry and Chemical Engineering, Queen's University of Belfast, Belfast, Ireland BT9 5AG, U.K.; Welcome-Wolfson Institute for Experimental Medicine, School of Medicine, Dentistry and Biomedical Sciences, The Queen's University Belfast, BT9 7BL Belfast, U.K..*

Complete contact information is available at: https://pubs.acs.org/10.1021/acssuschemeng.0c08586

Author Contributions

The manuscript was written through contributions of all authors. All authors have given approval to the final version of the manuscript.

Notes

The authors declare no competing financial interest.

■ ACKNOWLEDGMENTS

We thank the QUILL and University of Palermo for financial support (FFR 2018). F.B. gratefully acknowledges the GSK Carbon Neutral Laboratories of the University of Nottingham.

■ REFERENCES

(1) Weinstein, L. A.; Loomis, J.; Bhatia, B.; Bierman, D. M.; Wang, E. N.; Chen, G. Concentrating Solar Power. *Chem. Rev.* **2015**, *115*, 12797−12838.

(2) Zhang, H.; Baeyens, J.; Cáceres, G.; Degrève, J.; Lv, Y. Thermal energy storage: Recent developments and practical aspects. *Progr. Energy Combust. Sci.* **2016**, *53*, 1−40.

(3) Gur, I.; Sawyer, K.; Prasher, R. Searching for a Better Thermal Battery. *Science* **2012**, *335*, 1454−1455.

(4) Kucharski, T. J.; Tian, Y.; Akbulatov, S.; Boulatov, R. Chemical solutions for the closed-cycle storage of solar energy. *Energy Environ. Sci.* **2011**, *4*, 4449−4472.

(5) Gurke, J.; Quick, M.; Ernsting, N. P.; Hecht, S. Acid-catalysed thermal cycloreversion of a diarylethene: a potential way for triggered release of stored light energy? *Chem. Commun.* **2017**, *53*, 2150−2153.

(6) Huang, J.; Jiang, Y.; Wang, J.; Li, C.; Luo, W. A high energy, reusable and daily-utilization molecular solar thermal conversion and storage material based on azobenzene/multi-walled carbon nanotubes hybrid. *Thermochim. Acta* **2017**, *657*, 163−169.

(7) Jorner, K.; Dreos, A.; Emanuelsson, R.; El Bakouri, O.; Fdez Galván, I.; Börjesson, K.; Feixas, F.; Lindh, R.; Zietz, B.; Moth-Poulsen, K.; Ottosson, H. Unraveling factors leading to efficient norbornadiene−quadricyclane molecular solar-thermal energy storage systems. *J. Mater. Chem. A* **2017**, *5*, 12369−12378.

(8) Masutani, K.; Morikawa, M.-a.; Kimizuka, N. A liquid azobenzene derivative as a solvent-free solar thermal fuel. *Chem. Commun.* **2014**, *50*, 15803−15806.
(9) Saydjari, A. K.; Weis, P.; Wu, S. Spanning the Solar Spectrum: Azopolymer Solar Thermal Fuels for Simultaneous UV and Visible Light Storage. *Adv. Energy Mater.* **2017**, *7*, 1601622.
(10) Crano, J. C.; Guglielmetti, R. J. Organic Photochromic and Thermochromic Compounds. *Volume 2: Physicochemical Studies, Biological Applications, and Thermochromism*; Springer: United States, 2006.
(11) Andrews, D. L. *Energy Harvesting Materials*; World Scientific Publishing Ltd, 2005.
(12) Day, J. H. Thermochromism of inorganic compounds. *Chem. Rev.* **1968**, *68*, 649−657.
(13) Yuan, T.; Xu, Y.; Zhu, C.; Jiang, Z.; Sue, H.-J.; Fang, L.; Olson, M. A. Tunable Thermochromism of Multifunctional Charge-Transfer-Based Supramolecular Materials Assembled in Water. *Chem. Mater.* **2017**, *29*, 9937−9945.
(14) Kalninsh, K. K. Structure and thermochromism of spiropyrans. Triplet mechanism of the thermal cleavage/closure of the pyran ring. *J. Struct. Chem.* **1998**, *39*, 642−650.
(15) Sone, K.; Fukuda, Y. Thermochromic and Chromotropic Phenomena of Cobalt(II) Chloride Solutions and Related Systems. *Inorganic Thermochromism. Inorganic Chemistry Concepts*; Springer: Berlin, Heidelberg, 1987; Vol. *10*; pp 13−42.
(16) Kohno, Y.; Cowan, M. G.; Masuda, M.; Bhowmick, I.; Shores, M. P.; Gin, D. L.; Noble, R. D. A cobalt(ii) bis(salicylate)-based ionic liquid that shows thermoresponsive and selective water coordination. *Chem. Commun.* **2014**, *50*, 6633−6636.
(17) Barry, N. P. E.; Deeth, R. J.; Clarkson, G. J.; Prokes, I.; Sadler, P. J. Thermochromic organometallic complexes: experimental and theoretical studies of 16- to 18-electron interconversions of adducts of arene Ru(ii) carboranes with aromatic amine ligands. *Dalton Trans.* **2013**, *42*, 2580−2587.
(18) Garshasbi, S.; Santamouris, M. Using advanced thermochromic technologies in the built environment: Recent development and potential to decrease the energy consumption and fight urban overheating. *Sol. Energy Mater. Sol. Cells* **2019**, *191*, 21−32.
(19) Seeboth, A.; Ruhmann, R.; Mühling, O. Thermotropic and Thermochromic Polymer Based Materials for Adaptive Solar Control. *Materials* **2010**, *3*, 5143−5168.
(20) Binions, R. Thermochromic Thin Films and Nanocomposites for Smart Glazing. *Intelligent Nanomaterials*; Tiwari, A., Mishra, A. K., Kobayashi, H., Turner, A. P., Eds.; John Wiley & Sons, 2012; pp 251−316.
(21) Hoffmann, S.; Lee, E. S.; Clavero, C. Examination of the technical potential of near-infrared switching thermochromic windows for commercial building applications. *Sol. Energy Mater. Sol. Cells* **2014**, *123*, 65−80.
(22) Bamfiel, P.; Hutchings, M. *Chromic Phenomena: Technological Applications of Colour Chemistry*, 3rd ed.; Royal Society of Chemistry, 2018.
(23) Nieuwpoort, W. C.; Wesselink, G. A.; van der Wee, E. H. A. M. Thermochromic and solvochromic behaviour of cobalt (II) chloride solutions in various solvents. *Recl. Trav. Chim. Pays-Bas* **1966**, *85*, 397−404.
(24) Lei, Z.; Chen, B.; Koo, Y.-M.; MacFarlane, D. R. Introduction: Ionic Liquids. *Chem. Rev.* **2017**, *117*, 6633−6635.
(25) Shen, C.; Sheng, T.; Zhu, Q.; Hu, S.; Wu, X. Four new cobalt(ii) coordination complexes: thermochromic switchable behavior in the process of dehydration and rehydration. *CrystEngComm* **2012**, *14*, 3189−3198.
(26) D'Anna, F.; Nimal Gunaratne, H. Q.; Lazzara, G.; Noto, R.; Rizzo, C.; Seddon, K. R. Solution and thermal behaviour of novel dicationic imidazolium ionic liquids. *Org. Biomol. Chem.* **2013**, *11*, 5836−5846.
(27) Cruz, T. F. C.; Shimizu, K.; Esperança, J. M. S. S.; André, V.; Duarte, M. T.; Rebelo, L. P. N.; Gomes, P. T.; Canongia Lopes, J. N. Ionic Liquids in Wonderland: From Electrostatics to Coordination Chemistry. *J. Phys. Chem. C* **2019**, *123*, 5804−5811.
(28) Rizzo, C.; D'Anna, F.; Noto, R. Functionalised diimidazolium salts: the anion effect on the catalytic ability. *RSC Adv.* **2016**, *6*, 58477−58484.
(29) Rizzo, C.; Marullo, S.; Dintcheva, N. T.; Gambarotti, C.; Billeci, F.; D'Anna, F. Ionic liquid gels and antioxidant carbon nanotubes: Hybrid soft materials with improved radical scavenging activity. *J. Colloid Interface Sci.* **2019**, *556*, 628−639.
(30) Gu, C.-D.; Tu, J.-P. Thermochromic behavior of chloronickel(II) in deep eutectic solvents and their application in thermochromic composite films. *RSC Adv.* **2011**, *1*, 1220−1227.
(31) Wei, X.; Yu, L.; Jin, X.; Wang, D.; Chen, G. Z. Solar-thermochromism of Pseudocrystalline Nanodroplets of Ionic Liquid−NiII Complexes Immobilized inside Translucent Microporous PVDF Films. *Adv. Mater.* **2009**, *21*, 776−780.
(32) Wei, X.; Yu, L.; Wang, D.; Jin, X.; Chen, G. Z. Thermo-solvatochromism of chloro-nickel complexes in 1-hydroxyalkyl-3-methyl-imidazolium cation based ionic liquids. *Green Chem.* **2008**, *10*, 296−305.
(33) Banic, N.; Vranes, M.; Abramović, B.; Canadi, J.; Gadžurić, S. Thermochromism, stability and thermodynamics of cobalt(II) complexes in newly synthesized nitrate based ionic liquid and its photostability. *Dalton Trans.* **2014**, *43*, 15515−15525.
(34) May, B.; Hönle, M.; Heller, B.; Greco, F.; Bhuin, R.; Steinrück, H.-P.; Maier, F. Surface-Induced Changes in the Thermochromic Transformation of an Ionic Liquid Cobalt Thiocyanate Complex. *J. Phys. Chem. Lett.* **2017**, *8*, 1137−1141.
(35) McCourt, É.; Wojnarowska, Z.; Jacquemin, J.; Nockemann, P.; Manyar, H. G.; Hawelek, L.; Paluch, M. Temperature- and Pressure-Induced Structural Changes of Cobalt(II) in a Phosphonium-Based Ionic Liquid. *J. Phys. Chem. C* **2016**, *120*, 10156−10161.
(36) Osborne, S. J.; Wellens, S.; Ward, C.; Felton, S.; Bowman, R. M.; Binnemans, K.; Swadźba-Kwaśny, M.; Gunaratne, H. Q. N.; Nockemann, P. Thermochromism and switchable paramagnetism of cobalt(ii) in thiocyanate ionic liquids. *Dalton Trans.* **2015**, *44*, 11286−11289.
(37) Sniekers, J.; Geysens, P.; Vander Hoogerstraete, T.; Van Meervelt, L.; Fransaer, J.; Binnemans, K. Cobalt(ii) liquid metal salts for high current density electrodeposition of cobalt. *Dalton Trans.* **2018**, *47*, 4975−4986.
(38) Billeci, F.; Gunaratne, H. Q. N.; D'Anna, F.; Morgan, G. G.; Seddon, K. R.; Plechkova, N. V. A magnetic self-contained thermochromic system with convenient temperature range. *Green Chem.* **2019**, *21*, 1412−1416.
(39) Billeci, F.; D'Anna, F.; Feroci, M.; Cancemi, P.; Feo, S.; Forlino, A.; Tonnelli, F.; Seddon, K. R.; Gunaratne, H. Q. N.; Plechkova, N. V. When Functionalization Becomes Useful: Ionic Liquids with a "Sweet" Appended Moiety Demonstrate Drastically Reduced Toxicological Effects. *ACS Sustainable Chem. Eng.* **2020**, *8*, 926−938.
(40) Miessler, G. L.; Tarr, D. A. *Inorganic Chemistry*; Prentice Hall: New Jersey, 1998.
(41) Berlett, B. S.; Levine, R. L.; Stadtman, E. R. Use of Isosbestic Point Wavelength Shifts to Estimate the Fraction of a Precursor That Is Converted to a Given Product. *Anal. Biochem.* **2000**, *287*, 329−333.
(42) Hajime, M.; Masahiro, Y.; Kazumi, T.; Masakatsu, N.; Yukiko, K.; Yoshinori, M. Highly Conductive Room Temperature Molten Salts Based on Small Trimethylalkylammonium Cations and Bis(trifluoromethylsulfonyl)imide. *Chem. Lett.* **2000**, 922−923.
(43) Lee, C.-P.; Peng, J.-D.; Velayutham, D.; Chang, J.; Chen, P.-W.; Suryanarayanan, V.; Ho, K.-C. Trialkylsulfonium and tetraalkylammonium cations-based ionic liquid electrolytes for quasi-solid-state dye-sensitized solar cells. *Electrochim. Acta* **2013**, *114*, 303−308.
(44) Billeci, F.; D'Anna, F.; Gunaratne, H. Q. N.; Plechkova, N. V.; Seddon, K. R. "Sweet" ionic liquid gels: materials for sweetening of fuels. *Green Chem.* **2018**, *20*, 4260−4276.
(45) Marusak, R. A.; Doan, K.; Cummings, S. D. Werner's Notion—Creating the Field: Synthesis and Analysis of Cobalt Ammine

https://dx.doi.org/10.1021/acssuschemeng.0c08586
ACS Sustainable Chem. Eng. 2021, 9, 4064−4075

Coordination Compounds1−15. *Integrated Approach to Coordination Chemistry*; Wiley, 2006; pp 22−51.
(46) Sharutin, V. V.; Senchurin, V. S.; Sharutina, O. K.; Kunkurdonova, B. B. Synthesis and structure of cobalt complexes [Me3EtN]2+[CoI4]2− and [Me3BuN]2+[CoI4]2−. *Russ. J. Inorg. Chem.* **2011**, *56*, 1384−1389.
(47) Renny, J. S.; Tomasevich, L. L.; Tallmadge, E. H.; Collum, D. B. Method of continuous variations: applications of job plots to the study of molecular associations in organometallic chemistry. *Angew. Chem., Int. Ed.* **2013**, *52*, 11998−12013.
(48) Karlin, K. D. *Progress in Inorganic Chemistry*; Wiley: New York, 1982; Vol. *29*.
(49) Evans, D. F. 400. The determination of the paramagnetic susceptibility of substances in solution by nuclear magnetic resonance. *J. Chem. Soc.* **1959**, 2003−2005.
(50) Chauvin, Y.; Gilbert, B.; Guibard, I. Catalytic dimerization of alkenes by nickel complexes in organochloroaluminate molten salts. *J. Chem. Soc., Chem. Commun.* **1990**, 1715−1716.
(51) Cotton, F. A.; Wilkinson, G. *Advanced Inorganic Chemistry*, 3rd ed.; John Wiley: United States, 1972.
(52) Nicholls, D. 41-COBALT. *The Chemistry of Iron, Cobalt and Nickel*; Nicholls, D., Ed.; Pergamon: U.K., 1973; pp 1053−1107.
(53) McClintock, L. F.; Bagaria, P.; Kjaergaard, H. G.; Blackman, A. G. Co(III) complexes of the type [(L)Co(O2CO)]+ (L=tripodal tetraamine ligand): Synthesis, structure, DFT calculations and 59Co NMR. *Polyhedron* **2009**, *28*, 1459−1468.
(54) Medek, A.; Frydman, V.; Frydman, L. Solid and liquid phase 59Co NMR studies of cobalamins and their derivatives. *Proc. Natl. Acad. Sci. U.S.A.* **1997**, *94*, 14237−14242.
(55) Ozvat, T. M.; Peña, M. E.; Zadrozny, J. M. Influence of ligand encapsulation on cobalt-59 chemical-shift thermometry. *Chem. Sci.* **2019**, *10*, 6727−6734.
(56) Freeman, R.; Murray, G. R.; Richards, R. E.; Thompson, H. W. Cobalt nuclear resonance spectra. *Proc. R. Soc. London, Ser. A* **1957**, *242*, 455−466.
(57) Xu, Z.; Wang, S.; Hu, X.-Y.; Jiang, J.; Sun, X.; Wang, L. Sunlight-Induced Photo-Thermochromic Supramolecular Nanocomposite Hydrogel Film for Energy-Saving Smart Window. *Sol. RRL* **2018**, *2*, 1800204.
(58) Salamati, M.; Kamyabjou, G.; Mohamadi, M.; Taghizade, K.; Kowsari, E. Preparation of TiO2@W-VO2 thermochromic thin film for the application of energy efficient smart windows and energy modeling studies of the produced glass. *Constr. Build. Mater.* **2019**, *218*, 477−482.
(59) Liu, P.; Liu, L.; Jiang, K.; Fan, S. Carbon-Nanotube-Film Microheater on a Polyethylene Terephthalate Substrate and Its Application in Thermochromic Displays. *Small* **2011**, *7*, 732−736.
(60) Bavafa-Toosi, Y. 6-Nyquist plot. *Introduction to Linear Control Systems*; Bavafa-Toosi, Y., Ed.; Academic Press, 2019; pp 533−640.

https://dx.doi.org/10.1021/acssuschemeng.0c08586
ACS Sustainable Chem. Eng. 2021, 9, 4064−4075